

UCLA

UCLA Previously Published Works

Title

Transition State Gauche Effects Control the Torquoselectivities of the Electrocyclizations of Chiral 1-Azatrienes

Permalink

<https://escholarship.org/uc/item/9fs356wb>

Journal

The Journal of Organic Chemistry, 80(23)

ISSN

0022-3263

Authors

Patel, Ashay
Vella, Joseph R
Ma, Zhi-Xiong
[et al.](#)

Publication Date

2015-12-04

DOI

10.1021/acs.joc.5b02085

Peer reviewed



Published in final edited form as:

J Org Chem. 2015 December 04; 80(23): 11888–11894. doi:10.1021/acs.joc.5b02085.

Transition State *Gauche* Effects Control the Torquoselectivities of the Electrocyclizations of Chiral 1-Azatrienes

Ashay Patel[‡], Joseph R. Vella[‡], Zhi-Xiong Ma[§], R. P. Hsung[§], and K. N. Houk^{‡,¶}

[‡]Department of Chemistry and Biochemistry, University of California, Los Angeles, California, 90095, United States

[§]Division of Pharmaceutical Sciences, School of Pharmacy, and Department of Chemistry, University of Wisconsin, Madison, Wisconsin 53705, United States

[¶]Department of Chemical and Biomolecular Engineering, University of California, Los Angeles, California, 90095, United States

Abstract

Hsung *et al.* have reported a series of torquoselective electrocyclizations of chiral 1-azahexa-1,3,5-trienes that yield functionalized dihydropyridines. To understand the origins of the torquoselectivities of these azaelectrocyclizations, we modeled these electrocyclic ring closures using the M06-2X density functional. A new stereochemical model that rationalizes the observed 1,2 stereoselection emerges from these computations. This model is an improvement and generalization of the “*inside-alkoxy*” model used to rationalize stereoselectivities of 1,3-dipolar cycloaddition of chiral allyl ethers and emphasizes a stabilizing hyperconjugative effect, which we have termed a transition state *gauche* effect. This stereoelectronic effect controls the conformational preferences at the electrocyclization transition states, and only in one of the allowed, disrotatory electrocyclization transition states is the ideal stereoelectronic arrangement of substituent achieved without the introduction of a steric clash. Computational experiments confirm the role of this effect as a stereodeterminant, since substrates with electropositive groups like a silyl substituent and electronegative groups have different conformational preferences at the transition state and undergo ring closure with divergent stereochemical outcomes. This predicted reversal of stereoselectivity for the ring closure of a silyl-substituted azatriene has been demonstrated experimentally.

Graphical abstract

Correspondence to: R. P. Hsung; K. N. Houk.

SUPPORTING INFORMATION AVAILABLE: Experimental procedures, proton and carbon NMR spectra. Cartesian coordinates, zero point energy (ZPE), thermal and quasiharmonic corrections for all reported structures of all computed structures, as well as the imaginary frequencies of transition states. This information is available free of charge via the Internet at <http://pubs.acs.org>.



Introduction

Hsung *et al.* have demonstrated that an allylic stereocenter can influence the stereochemical outcomes of the disrotatory 6π electrocyclizations of substituted 1-aza-1,3Z,5-hexatrienes (summarized in Scheme 1).¹ Here we report – on the basis M06-2X/6–31+G(d,p) computations – that *gauche* effects present in the electrocyclization transition states determine the preferred mode of disrotatory ring closure for these chiral 1-azatrienes. In short, the forming C–N bond prefers to maintain a *gauche* relationship with the C–O bond at the allylic stereocenter.

Ring closures of azatrienes have been examined by a number of researchers^{2–13} and examples of stereoselective azaelectrocyclizations^{14–21} have been reported. Despite the utility of the 6π electrocyclization in natural product synthesis and even in biological contexts (i.e., covalent enzyme inhibition and biolabeling),^{22,23} the origins of the torquoselectivities of these electrocyclizations have yet to be understood. Previous experimental work suggests electrocyclizations of 1-azatrienes are often reversible at elevated temperatures,³ unlike the 6π electrocyclization of 1,3Z,5-hexatriene. However, experiments suggest that azatrienes shown in Scheme 1 undergo irreversible ring closure;¹ hence, the stereoselectivities of these reactions are under kinetic control.

Results and Discussion

Figure 1 illustrates the allowed disrotatory transition structures of the ring closures of 1,3,5-hexatriene **1** and those of its 1-aza analogue **2**. Whereas the electrocyclization of 1,3,5-hexatriene proceeds through a C_s symmetric boat-like geometry, the transition structures for the corresponding azaelectrocyclization are of lower symmetry; the structures are distorted such that the nitrogen of the azatriene appears to “approach” the *C*-terminus of the azatriene from above or below the plane of the terminal double bond. According to our previous work, this distortion allows the lone pair of the imine nitrogen to overlap with triene π system, stabilizing the transition state. Lone pair conjugation of this sort is largely responsible for $\sim 10^7$ -fold (at 298.15 K, see Figure 1 for free energies of activation) increase in reactivity of 1-azahexa-1,3,5-triene relative to 1,3,5-hexatriene.²⁴

1-azatriene **3** is representative of the substrates examined by Hsung and coworkers.¹ It features a number of C–C single bonds capable of free rotation; thus, to reduce the number of conformations that needed to be sampled we examined the simplified trienes, **5a–c**, **6**, and **7**, shown in Scheme 2. In all cases, three rotameric transition states were found for each of the disrotatory modes of ring closure (see Figure 2). We labeled these transition states based on the position of the alkoxy substituent with respect the terminal alkene of the azatriene,

nomenclature previously used to describe stereoselective additions to alkenes bearing allylic stereocenters.²⁵

For both disrotatory modes of ring closure of **5a**, the transition states in which the alkoxy substituent in the *inside* position (see Figure 2) are most stable. A *gauche* effect is responsible for this conformational preference. In the **TS5a_{in1}** and **TS5a_{in2}**, the forming C–N bond and the C–O bond between the alkoxy substituent and the allylic stereocenter are antiperiplanar to σ -donating bonds (C–C and C–H bonds, respectively) and *gauche* to one another. The *anti* transition state conformers **TS5a_{anti1}** and **TS5a_{anti2}**, which do not have these favorable donor-acceptor interactions, and are both about 2 kcal mol⁻¹ higher in energy. The *outside*-alkoxy transition states (**TS5a_{out1}** and **TS5a_{out2}**) also have a *gauche* arrangement of the C–O and forming C–N bonds and as a result are more stable than the *anti* transition structures. However, these transition structures are higher in energy than **TS5a_{in1}** and **TS5a_{in2}** due to electrostatic repulsion between the oxygen of the alkoxy group and the azatriene nitrogen. The O–N interatomic distances are shorter in the outside transition state conformer than the corresponding inside transition structures.

The *gauche* effect described above differs from a ground state *gauche* effect^{26,27} in that one of the C–X σ acceptors is a bond that is only partially formed in the transition state. For this reason, we have termed this hyperconjugative effect a “transition state *gauche* effect”. For these chiral azatrienes, it is the *gauche* relationship between forming C–N and the vicinal C–X bonds at the allylic position of the triene that is ultimately responsible for stereoselection (Scheme 3). Transition state *gauche* effects of this type are likely general phenomena, and may be responsible for the stereoselectivity of other reactions involving alkenes that possess an allylic σ acceptor. The “inside-alkoxy” effect invoked by Houk^{25,28–31} and others³² to rationalize the stereoselectivities of 1,3-dipolar cycloadditions of nitrones and nitrile oxides and chiral allyl ethers is now recognized to be one case of this more general stereochemical model.

To confirm that these stereoelectronic effects are the principal determinants of the transition state conformational preferences of these azaelectrocyclizations, we also modeled the transition states of related substrates **5b** and **5c**, bearing a fluorine or a silyl substituent at the stereogenic center, respectively. If these effects were important, then **5b** (R = F) should have conformational preferences qualitatively similar to those of **5a** at the transition state. Since the SiMe₃ group is a hyperconjugative donor³³, the *anti* transition state conformers of 1-azatriene **5c** should be the most stable: A good donor (C–Si σ bond) is antiperiplanar to electron-deficient forming C–N bond in the *anti* transition states of **5c**. The G^\ddagger of all six transition state conformers of **5a–c** are summarized in Figure 3.

The conformational preferences of the transition states of **5b** are, indeed, similar to those preferences observed for the transition states of **5a**. The *inside* transition states **TS5b_{in1}** and **TS5b_{in2}** are most stable, and the *anti* transition states are highest in energy. By contrast, we find that the *anti* transition state conformers are preferred for the ring closure of **5c** (R = SiMe₃), confirms the nature of C–N forming bond at the transition state as hyperconjugative acceptor. This *anti* preference is related to Cieplak’s rationalization regarding the origins of π -facial selectivity of nucleophilic additions to cyclic ketones,^{34,35} and suggests the nature

of bond formation in the electrocyclicization, a pericyclic process, is fundamentally different from bond formation in a polar reaction (e.g., nucleophilic acyl addition) for which Cieplak's rationale has been criticized.^{36,37}

Experimentally, Hsung et al. have demonstrated that the diastereoselectivities of these azaelectrocyclizations are sensitive to the nature of the N-substituent. To probe this effect, we first examined the transition states conformers of azatriene **6**, bearing a *N*-methyl substituent, and, then, cyclic azatriene **7**. The conformational preferences of **6** remain the same as those found for substrates **5a** and **5b**. According to computations, the two diastereomeric *inside* transition states of azatriene **6** differ in free energy by 1.0 kcal mol⁻¹ and are shown in Figure 4. This difference in G^\ddagger is consistent with the sense and level of diastereoselectivity observed experimentally and is caused by a steric clash that destabilizes **TS6_{in2}**. In **TS6_{in2}**, for the methoxy substituent to occupy its preferred *inside* position, the geminal methyl group must adopt the more sterically demanding *outside* position; whereas, in **TS6_{in1}** the hydrogen occupies the *outside* position when the alkoxy is in the *inside* arrangement. That this steric clash involves the *N*-methyl group explains the substituent's importance in stereinduction.

We next modeled the ring closure of a cyclic azatriene, compound **7**, (see Figure 5), which more closely resembles the experimental azatriene **4**. The reaction of the cyclic azatriene **7** proceeds with a barrier of almost 18 kcal mol⁻¹ and yields a product that is 16 kcal mol⁻¹ more stable than the reactant. Azatriene **7** is more than 10³-fold more reactive at room temperature ($G^\ddagger = 5$ kcal mol⁻¹) than **2a** due to activation by the carbonyl moiety of the lactone and restriction of a rotational degree of freedom by the fused lactone ring. For azatriene **7**, the outside transition states for either mode of ring closure are slightly more stable than the corresponding inside transition states. The subtle change of the conformational preference is due to A^{1,3} strain between the methylene group of the lactone and *N*-methyl of the azatriene in the inside transition state conformers of **7**. Nonetheless, a strong preference for a *gauche* conformation over the *anti* conformation is still predicted. The lowest energy conformers of either mode of disrotation differ by a G^\ddagger of ~1 kcal mol⁻¹, consistent with the observed diastereoselectivity for the reaction of **3**.

Finally, we return to the silyl derivative **5c**. As discussed above, the silyl group at the allylic position of the azatriene is predicted to reverse the stereoselectivity of the ring closure. This prediction inspired the syntheses and studies of the ring closures of chiral silyl-substituted 1-azatrienes, including, **10** (see Scheme 4). The synthesis of silyl-substituted 1-azatrienes and the scope of the ring closures of these compounds are reported separately.³⁸ The predicted stereochemical outcome is observed experimentally; however, the ring closure of 1-azatriene **10** is reversible at 130°C, and over time the diastereoselectivity of the reaction comes under thermodynamic control. Here we report the origins of the selectivity of the electrocyclicization of **10**, using azatriene **12** as a computational model substrate.

Just as is the case for the electrocyclicization of **5c**, the *anti* transition state conformers of the ring closure of **12** are lowest in energy. Hyperconjugative stabilization by interaction of the C–Si σ donor orbital with the antibonding σ^* orbital of the forming C–N bond is likely reinforced by the steric preference of the silyl group for the *anti* position. Computations of

the electrocyclic reaction of **12** are consistent with the experimental stereoselectivity; the computed kinetic product **13b** ($\Delta G^\ddagger = 2.0 \text{ kcal mol}^{-1}$) corresponds (in terms of relative stereochemistry) to dihydropyridine **11a**.³¹ The kinetic diastereoselectivity of the azaelectrocyclization of **12** is also controlled by a steric effect. In **TS12_{anti1}**, which leads to the minor product, the methyl substituent at the α position must adopt the *outside* position in order for the TMS group to occupy the *anti* position. In doing so, this methyl group clashes with the *N*-substituent. This clash is avoided in the favored transition structure **TS12_{anti2}** as the methyl and TMS groups are able to simultaneously occupy the less sterically demanding *inside* and *anti* positions, respectively.

The equilibration of the two diastereomeric electrocyclization products **13a** and **13b** is observed experimentally, although the major product is still **13b**. The computed $t_{1/2}$ at 130 °C for the ring opening (retroelectrocyclization) of either electrocyclization product is approximately 420 hr, too large a value considering experimental equilibration of the diastereomeric products of electrocyclization occurs within 24 hrs.³⁸ The bulky TBDPS group employed experimentally likely accelerates equilibration by destabilizing the products of the electrocyclic ring closure. In any case, the relative energy differences between two the dihydropyridine products indicate that the thermodynamic product is also the kinetic product **13a**.

Conclusions

Transition state *gauche* effects explain the observed stereoselectivities of the electrocyclizations of chiral 1-azatrienes bearing α -alkoxy substituents. Computational experiments predict that an allylic fluorine substituent at the allylic position reproduces the experimentally observed stereoselectivity, while a silyl group at the same position changes the preferred transition state conformation and reverses the stereochemical course of the ring closure. The electrocyclization of TBPDS-substituted azatriene **12** confirms this predicted reversal of selectivity. Studies of the generality of the stereochemical influence of α -silyl groups and the synthetic utility of the ring closures of α -silyl azatrienes have been reported separately.³⁸

Computational Methods

The DFT computations were performed using *Gaussian09*.³⁹ The M06-2X⁴⁰/6-31+G(d,p) model chemistry was used to optimize the geometries of stationary points and to compute the vibrational frequencies. M06-2X has been demonstrated to reliably reproduce the thermodynamics of π to σ transformations with reasonable accuracy⁴¹ in addition to the kinetics of main group chemistry.⁴² All computations were performed in the gas phase. Normal mode analysis confirmed that the optimized structures of reactants and products were minima (zero imaginary frequencies) and that all optimized transition structures corresponded to first-order saddle points (one imaginary frequency). Thermal corrections were calculated from unscaled M06-2X/6-31+G(d,p) frequencies using the standard state conditions of 1 atm and 298.15 K. Errors in the calculation of vibrational entropy contributions to the free energies by the treatment of low modes as harmonic vibrations was mitigated by raising the frequencies of vibrational modes less than 100 cm^{-1} to exactly 100

cm⁻¹ as suggested by Truhlar.^{43,44} Electronic energies were recomputed at the M06-2X/def2-QZVPP^{45,46} level of theory. Reported Gibbs free energies were determined using these electronic energies and thermal corrections determined at the M06-2X/6-31+G(d,p) level. The *Avogadro*^{47,48} and *Gaussview*⁴⁹ software packages were used to build and visualize molecules; the images used in this article were prepared with *CYLview*.⁵⁰ All energies reported are Gibbs free energies in kcal mol⁻¹.

Supplementary Material

Refer to Web version on PubMed Central for supplementary material.

Acknowledgments

We acknowledge the financial support of the NIH (GM-36700 and CHE-1351104 to K.N.H.) A.P. thanks the Chemical-Biology Interface Training Program for its support (T32 GM 008496). A.P and J.V acknowledge the University of California, Los Angeles and the Amgen Scholars Program, respectively, for financial support. The following computational resources were used in this study: the Hoffman2 cluster at UCLA (IDRE) and the Extreme Science and Engineering Discovery Environment (XSEDE)'s Trestles and Gordon supercomputers (OCI-1053575) at the San Diego Supercomputing Center.

References

1. Sydorenko N, Hsung RP, Vera EL. *Org Lett.* 2006; 8:2611. [PubMed: 16737326]
2. Gilchrist TL, Healy MAM. *Tetrahedron.* 1993; 49:2543.
3. Maynard DF, Okamura WH. *J. Am. Chem. Soc.* 1995; 60:1763.
4. Smith DA, Ulmer CW II. *J. Org. Chem.* 1991; 56:4444.
5. Beccalli EM, Clerici F, Gelmi ML. *Tetrahedron.* 2000; 56:4817–4821.
6. Palacios F, Gil MJ, de Marigorta EM, Rodríguez M. *Tetrahedron.* 2000; 56:6319.
7. Tanaka K, Katsumura S. *J. Synth. Org. Chem. Jpn.* 2005; 63:696.
8. Vincze Z, Mucsi Z, Scheiber P, Nemes P. *Eur. J. Org. Chem.* 2008:2008–1092.
9. Liu S, Liebeskind LS. *J. Am. Chem. Soc.* 2008; 130:6918. [PubMed: 18465855]
10. Nakamura I, Zhang D, Terada M. *J. Am. Chem. Soc.* 2010; 132:7884. [PubMed: 20469867]
11. Nakamura I, Zhang D, Terada M. *J. Am. Chem. Soc.* 2011; 133:6862.
12. Vincze Z, Nemes P. *Tetrahedron.* 2013; 69:6269.
13. For a review on aza-electrocyclizations: Okamura WH, de Lera AR. *Comprehensive Organic Synthesis.* Trost BM, Fleming I, Paquette LA. Pergamon Press New York 1991; 5:699–750.
14. Sklenicka HM, Hsung RP, Wei L-L, McLaughlin MJ, Gerasyuto AI, Degen SJ. *Org. Lett.* 2000; 2:1161. [PubMed: 10804579]
15. Tanaka K, Mori H, Yamamoto M, Katsumura S. *J. Org. Chem.* 2001; 66:3099. [PubMed: 11325275]
16. Tanaka K, Katsumura S. *J. Am. Chem. Soc.* 2002; 124:9660. [PubMed: 12175196]
17. Buchanan GS, Dai H, Hsung RP, Gerasyuto AI, Scheinebeck CM. *Org. Lett.* 2011; 13:4402. [PubMed: 21786757]
18. Thompson S, Coyne AG, Knipe PC, Smith MD. *Chem. Soc. Rev.* 2011; 40:4217. [PubMed: 21566810]
19. Sklenicka HM, Hsung RP, McLaughlin MJ, Wei LI, Gerasyuto AI, Brennessel WB. *J. Am. Chem. Soc.* 2002; 124:10435. [PubMed: 12197745]
20. Tanaka K, Kobayashi T, Mori H, Katsumura S. *J. Org. Chem.* 2004; 69:5906. [PubMed: 15373476]
21. Liu X, Zhang N, Yang J, Liang Y, Zhang R, Dong D. *J. Org. Chem.* 2013; 78:3323. [PubMed: 23445321]

22. Tanaka K, Yokoi S, Morimoto K, Iwata T, Nakamoto Y, Nakayama K, Koyama K, Fujiwara T, Fukase K. *Biorg. Med. Chem.* 2012; 20:1865.
23. Tanaka K, Fukase K, Katsumura S. *Chem. Rec.* 2010; 10:119. [PubMed: 20349508]
24. Walker MJ, Hietbrink BN, Thomas BE, Nakamura K, Kallel EA, Houk KN. *J. Org. Chem.* 2001; 66:6669. [PubMed: 11578219]
25. Houk KN, Moses SR, Wu YD, Rondan NG, Jager V, Schohe R, Fronczek FR. *J. Am. Chem. Soc.* 1984; 106:3880.
26. Wiberg KB, Murcko MA, Laidig KE, MacDougall PJ. *J. Phys. Chem.* 1990; 94:6956.
27. Goodman L, Gu HB, Pophristic V. *J. Phys. Chem. A.* 2005; 109:1223. [PubMed: 16833433]
29. Houk KN, Duh HY, Wu YD, Moses SR. *J. Am. Chem. Soc.* 1986; 106:2754.
29. Raimondi L, Wu YD, Brown FK, Houk KN. *Tetrahedron Lett.* 1992; 33:4409.
30. Haller J, Strassner T, Houk KN. *J. Am. Chem. Soc.* 1997; 62:8031.
31. Haller J, Niwayama S, How-Yunn Duh A, Houk KN. *J. Org. Chem.* 1997; 62:5728.
32. Annunziata R, Benaglia M, Cinquini M, Cozzi F, Raimondi L. *Eur. J. Org. Chem.* 1998; 1998:1823.
33. Lambert JB, Zhao Y, Emblidge RW, Salvador LA, Liu XY, So JH, Chelius EC. *Acc. Chem. Res.* 1999; 32:183.
34. Cieplak AS. *J. Am. Chem. Soc.* 1981; 103:4540.
35. Cieplak AS, Tait BD, Johnson CR. *J. Am. Chem. Soc.* 1989; 111:8447.
36. Wu YD, Houk KN. *J. Am. Chem. Soc.* 1987; 109:908.
37. Houk KN. *Chem. Rev.* 1976; 76:1.
38. Ma Z-X, Patel A, Houk KN, Hsung RP. *Org Lett.* 2015; 17:2138. [PubMed: 25859907]
39. Frisch MJ, Trucks GW, Schlegel HB, Scuseria GE, Robb MA, Cheeseman JR, Scalmani G, Barone V, Mennucci B, Petersson GA, Nakatsuji H, Caricato M, Li X, Hratchian HP, Izmaylov AF, Bloino J, Zheng G, Sonnenberg JL, Hada M, Ehara M, Toyota K, Fukuda R, Hasegawa J, Ishida M, Nakajima T, Honda Y, Kitao O, Nakai H, Vreven T, J A Montgomery J, Peralta JE, Ogliaro F, Bearpark M, Heyd JJ, Brothers E, Kudin KN, Staroverov VN, Kobayashi R, Normand J, Raghavachari K, Rendell A, Burant JC, Iyengar SS, Tomasi J, Cossi M, Rega N, Millam JM, Klene M, Knox JE, Cross JB, Bakken V, Adamo C, Jaramillo J, Gomperts R, Stratmann RE, Yazyev O, Austin AJ, Cammi R, Pomelli C, Ochterski JW, Martin RL, Morokuma K, Zakrzewski VG, Voth GA, Salvador P, Dannenberg JJ, Dapprich S, Daniels AD, Farka Ó, Foresman JB, Ortiz JV, Cioslowski J. *Gaussian 09, Revision D.01.*
40. Zhao Y, Truhlar DG. *Theor. Chem. Account.* 2008; 120:215.
41. Pieniazek SN, Clemente FR, Houk KN. *Angew. Chem. Int. Ed.* 2008; 120:7860.
42. Zhao Y, Truhlar DG. *Acc. Chem. Res.* 2008; 41:157. [PubMed: 18186612]
43. Zhao Y, Truhlar DG. *Phys. Chem. Chem. Phys.* 2008; 10:2813. [PubMed: 18464998]
44. Ribeiro RFR, Marenich AVA, Cramer CJC, Truhlar DGD. *J Phys Chem B.* 2011; 115:14556. [PubMed: 21875126]
45. Weigend F, Ahlrichs R. *Phys. Chem. Chem. Phys.* 2005; 7:3297–3305. [PubMed: 16240044]
46. Weigend F. *Phys. Chem. Chem. Phys.* 2006; 8:1057–1065. [PubMed: 16633586]
47. Hanwell MD, Curtis DE, Lonie DC, Vandermeersch T, Zurek E, Hutchison GR. *J Cheminform.* 2012; 4:17. [PubMed: 22889332]
48. Avogadro: an open-source molecular builder and visualization tool version 1.1.1; <http://avogadro.openmolecules.net/>.
49. Dennington, RoyKeith, Todd, Millam, John, editors. *GaussView, Version 5.* SemicheM Inc.; Shawnee Mission KS: 2009.
50. Legault, CY., editor. *CYLview, 1.0b.* Université de Sherbrooke; 2009. (<http://www.cylview.org>)

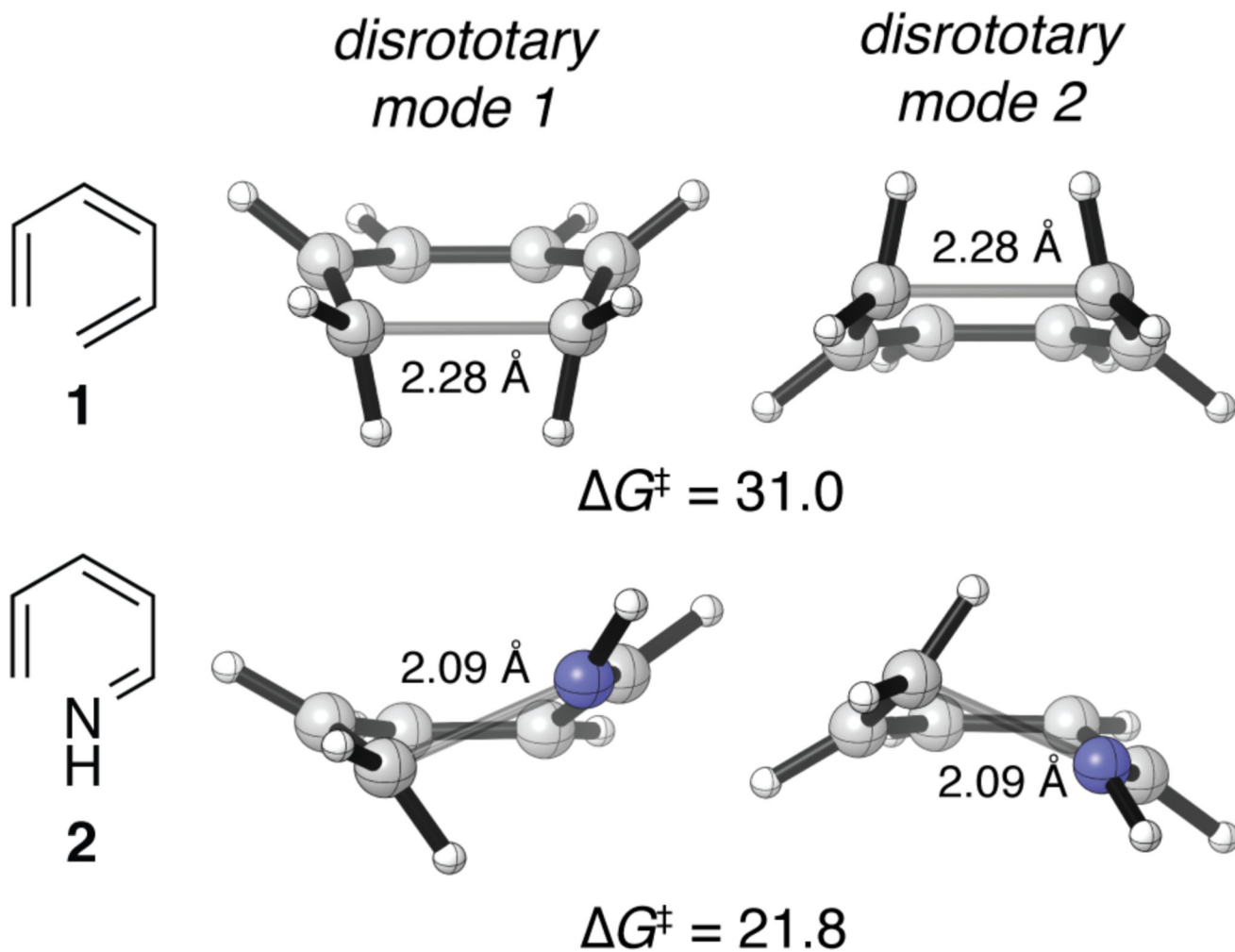


Figure 1. The thermally allowed disrotatory transition structures and activation free energies of the ring closures of 1,3,5-hexatriene and 1-azahexa-1,3,5-triene. Energies are Gibbs free energies in kcal mol⁻¹.

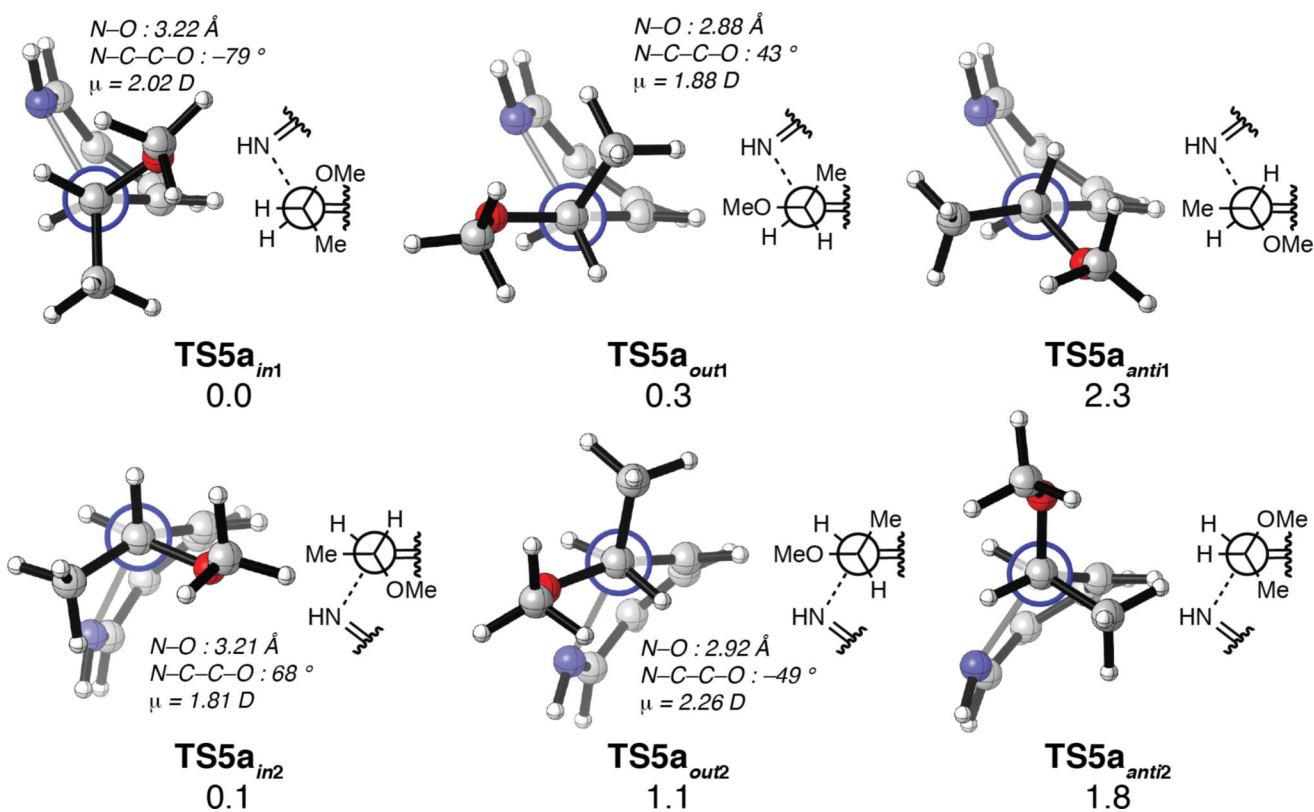
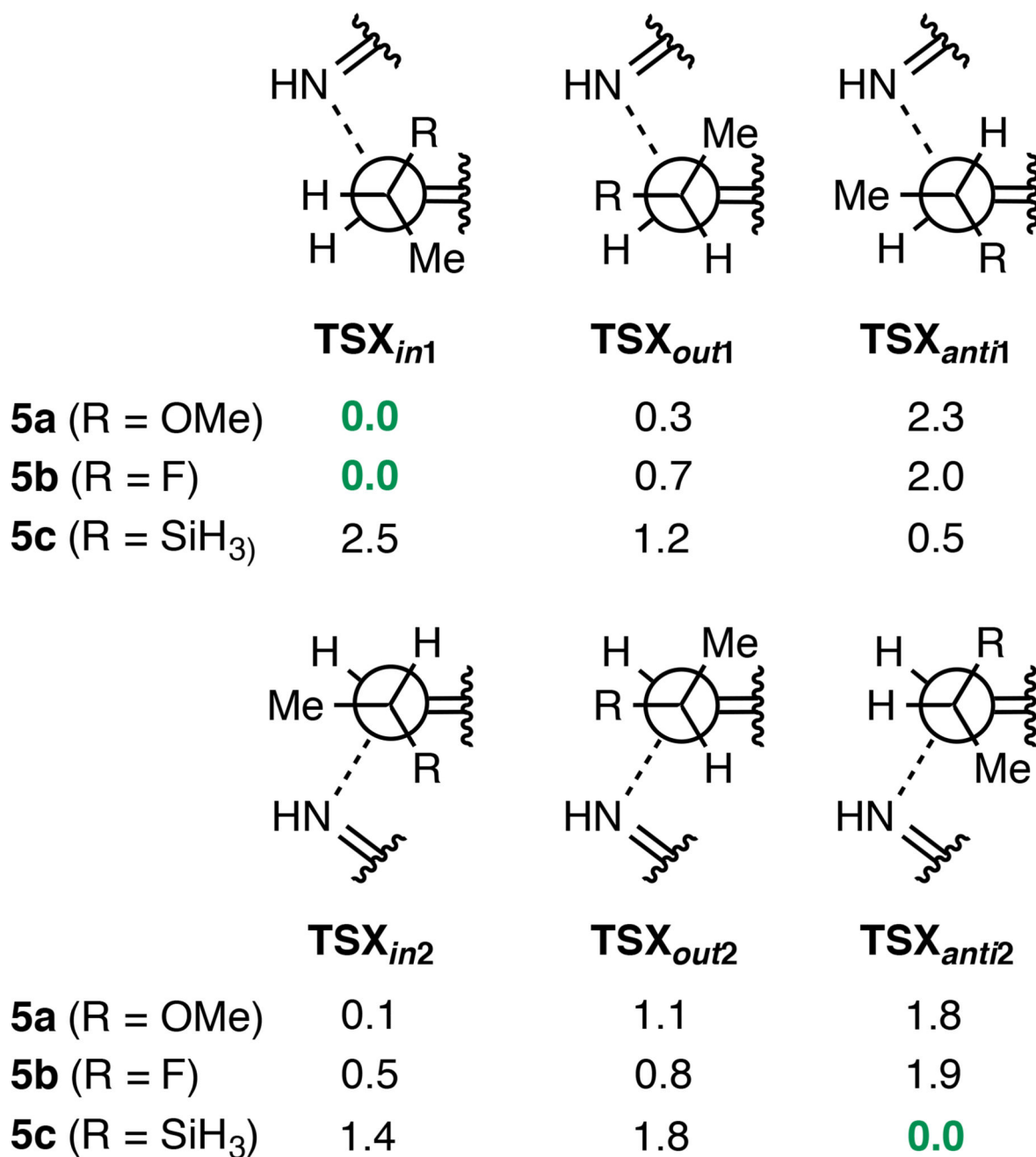


Figure 2. Newman projections of the C5–C6 bond of the M06-2X/6–31+G(d,p)-optimized transition state conformers for the ring closure of **5a**. G^\ddagger values are reported in kcal mol⁻¹.

**Figure 3.**

G^\ddagger differences of the M06-2X/6-31+G(d,p) optimized ring closure transition state conformers of **5a–c**. G^\ddagger values were determined relative to inside **TS_{dis1}** for the transition structures of azatrienes **5a** and **5b** and relative to **TS_{dis2}** for the transition structures of **5c**. Energies are reported in kcal mol⁻¹.

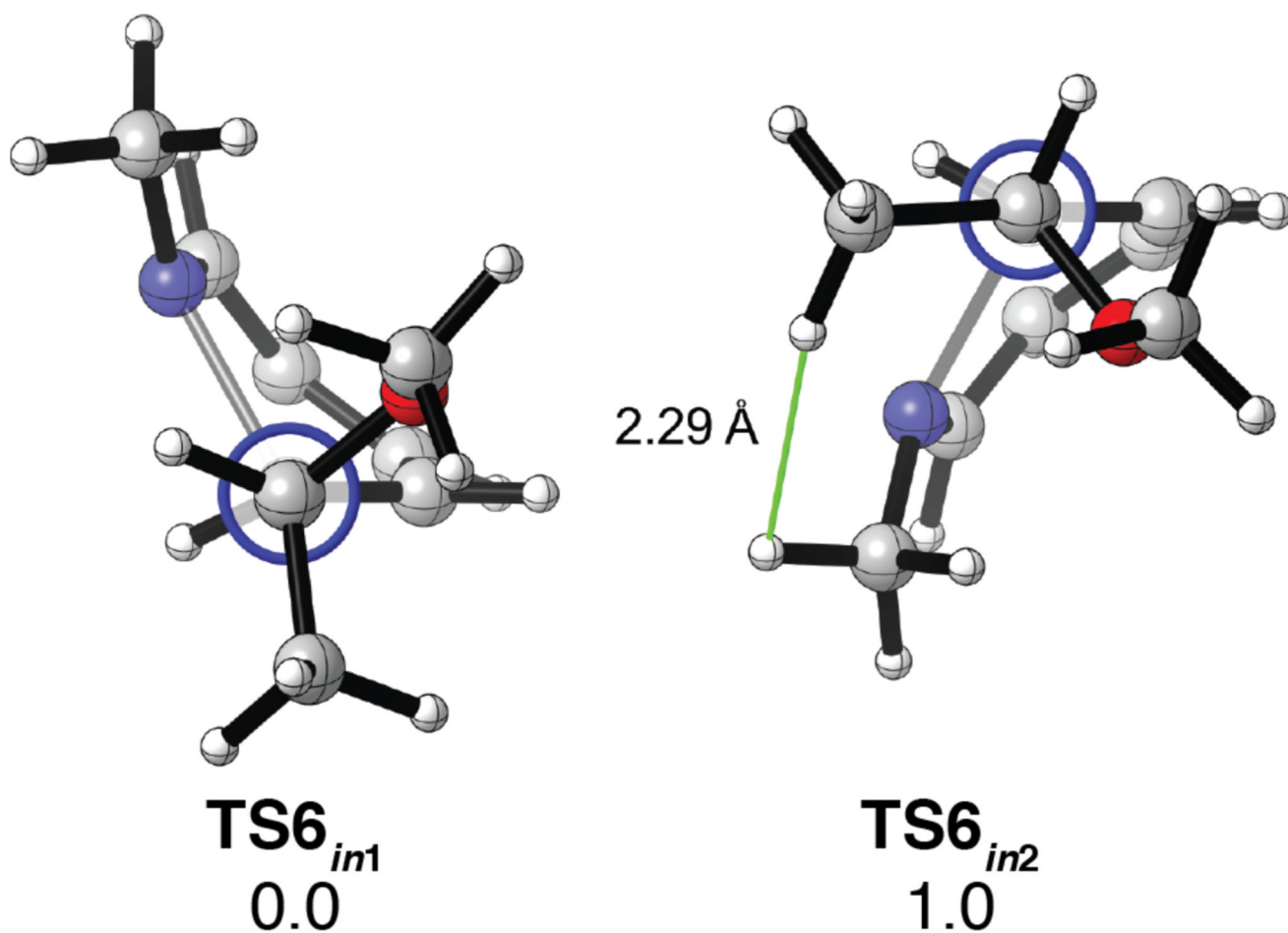


Figure 4. Newman projections of the lowest energy M06-2X/6-31+G(d,p)-optimized 6 π electrocyclic transition state conformers of **6**. G^\ddagger values are given in kcal mol⁻¹.

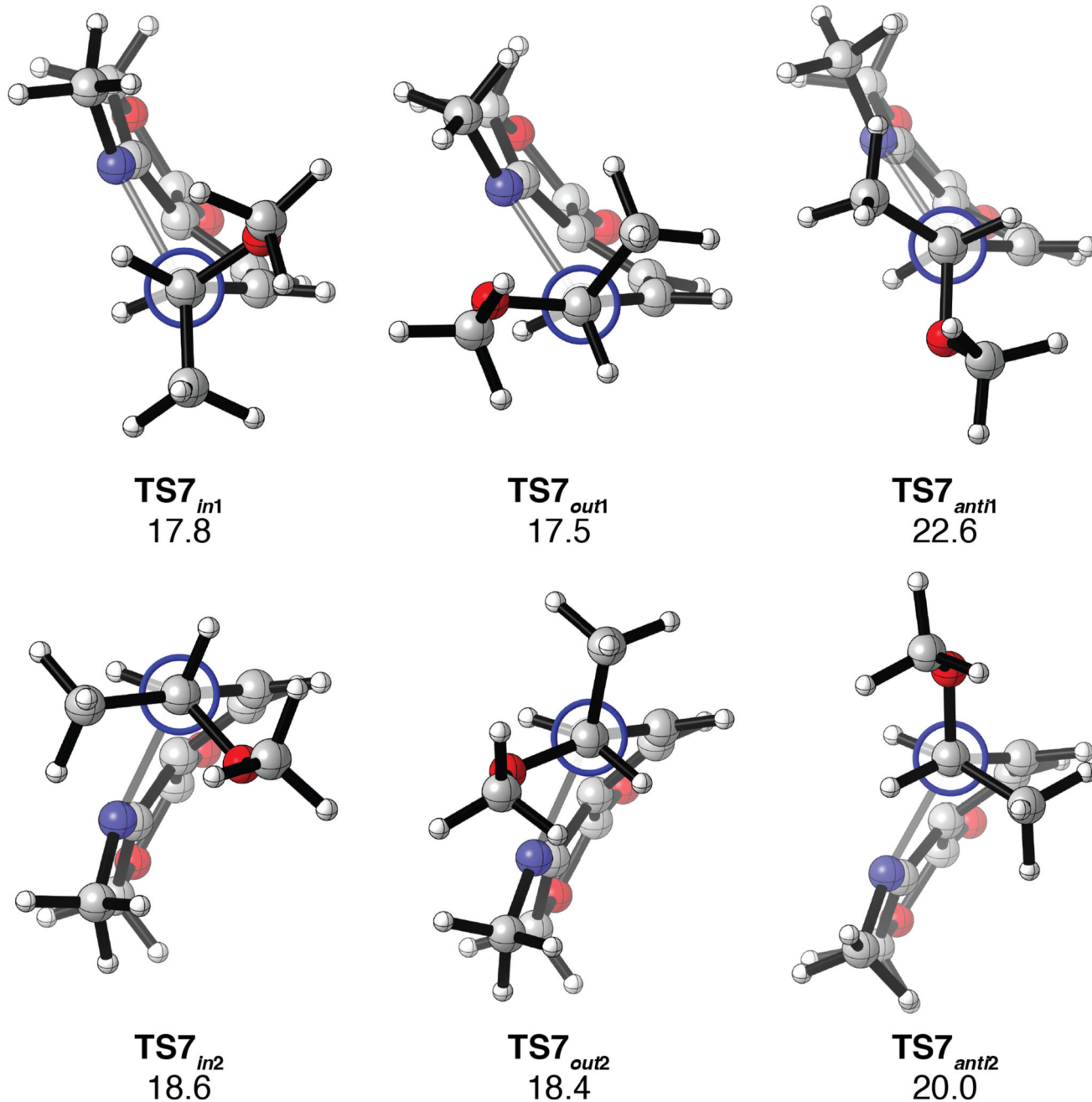


Figure 5. Newman projections of M06-2X/6-31+G(d,p) optimized transition state conformers of the 6π electrocyclicization of azatriene **7**. G^\ddagger are given in kcal mol^{-1} .

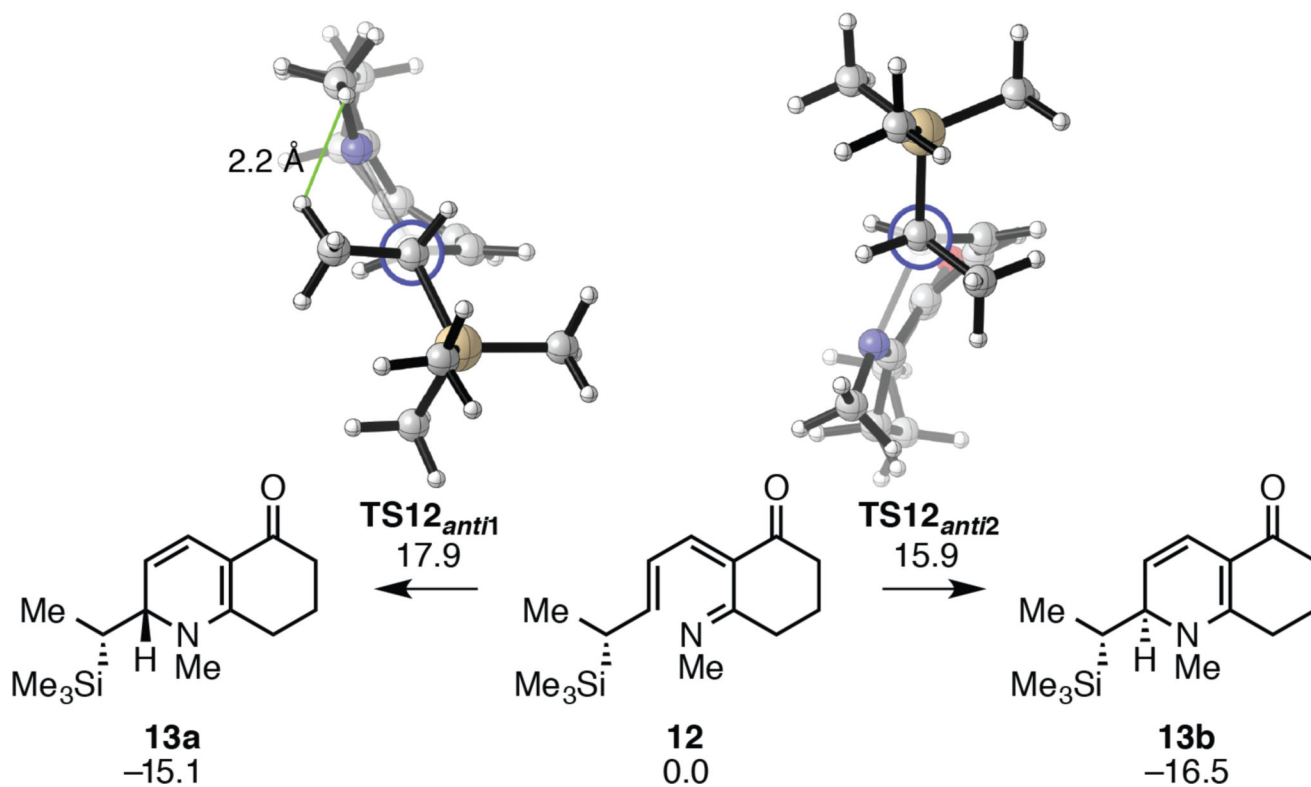
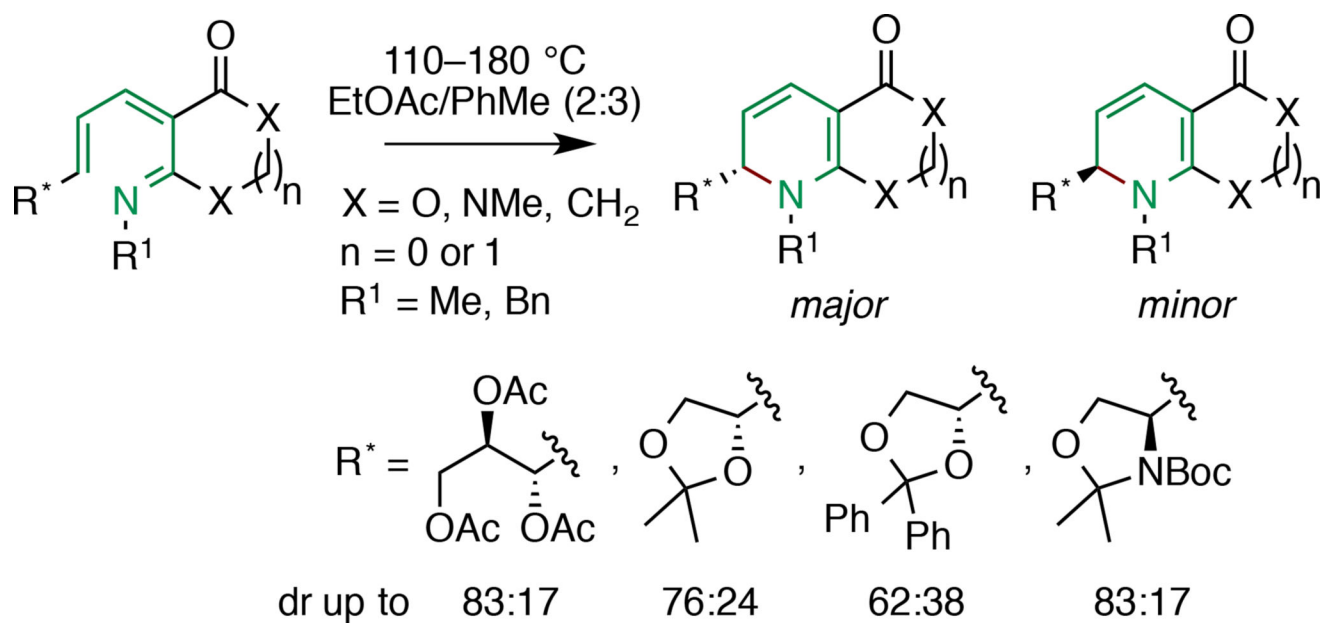
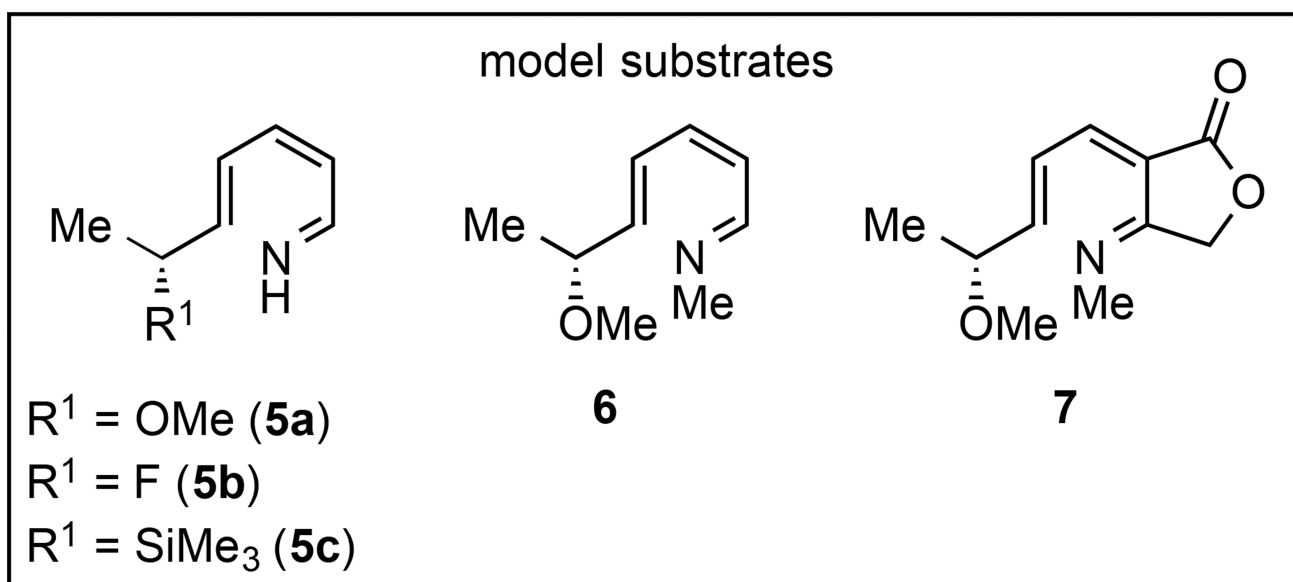
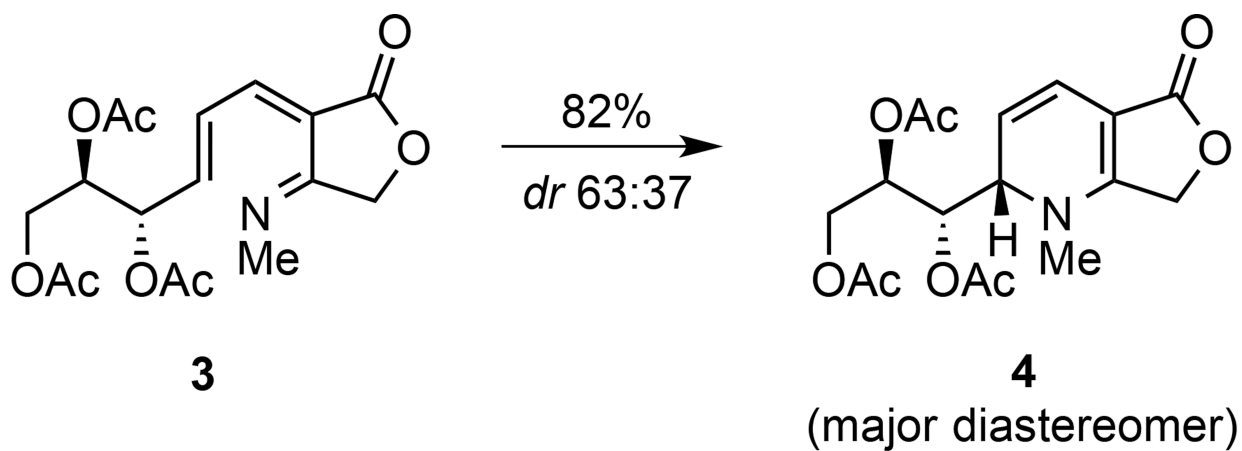


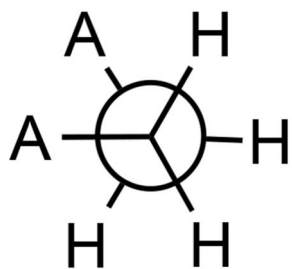
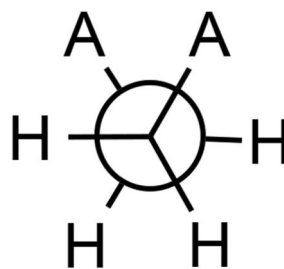
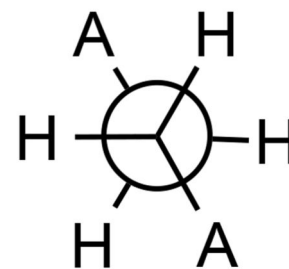
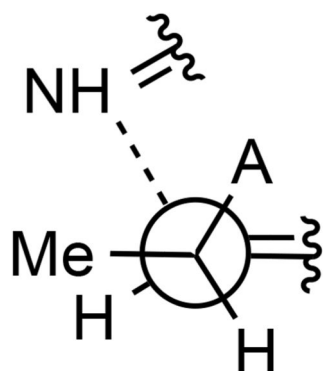
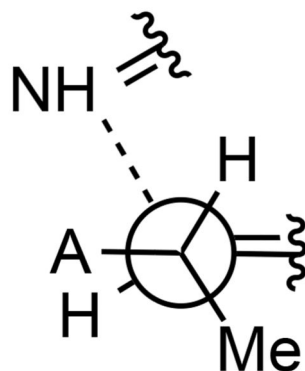
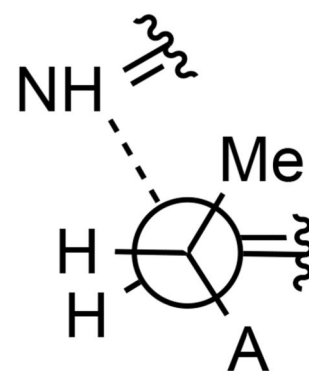
Figure 6. M06-2X/6-31+G(d,p)-optimized transition structures, G^\ddagger , and G_{rxn} for the electrocyclicization of **12**. Reported energies are in kcal mol⁻¹.

**Scheme 1.**

Torquoselective electrocyclizations of 1-aza-1,3Z,5-hexatrienes

**Scheme 2.**

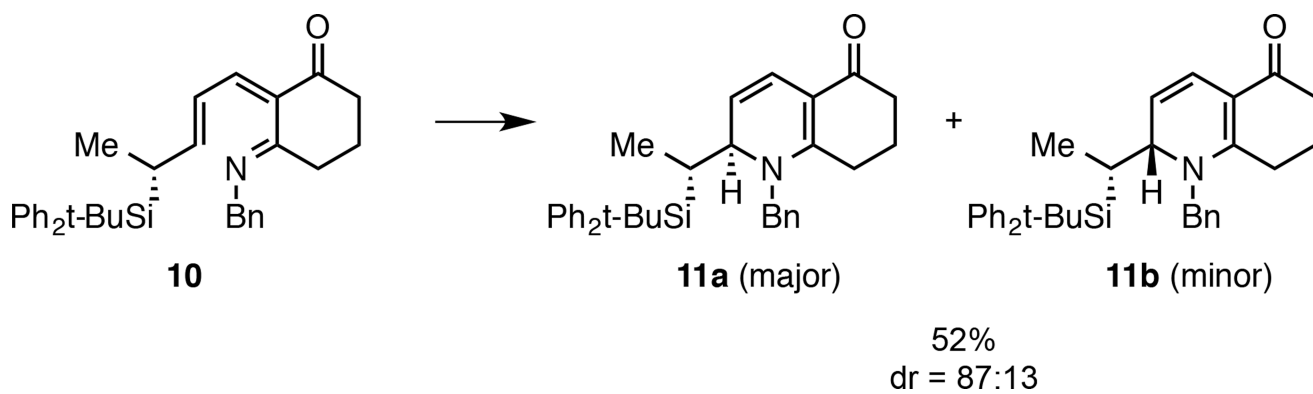
A representative azaelectrocyclization and model substrates examined computationally.

ground state *gauche* effect*gauche (+)**gauche (-)**anti*transition state *gauche* effect*gauche (TS_{in})**gauche (TS_{out})**anti (TS_{anti})*

two stabilizing acceptor-donor interactions
 no stabilizing acceptor-donor interactions

Scheme 3.

Newman projections illustrating the ground state and transition state *gauche* effects.

**Scheme 4.**

The electrocyclization of TBPDS-substituted 1-azatriene **10**.³¹